On the Modelling Aspect of Low-Velocity Impact Composite Laminates

M.S. Meon[*], *N.H. Mohamad Nor, S. Shawal, J.B. Saedon*
Faculty of Mechanical Engineering, Universiti Teknologi MARA (UiTM), 40450 Shah Alam, Selangor, Malaysia
**msuhairil@uitm.edu.my*

M.N. Rao, K.-U. Schröder
Institute for Structural Mechanics and Lightweight Design, RWTH Aachen University, Germany

ABSTRACT

Composites suffer a degradation of structural stiffness due to various types of impact loading resulting in damage which is difficult to observe from the surface of the structure. The paper deals with the finite element model (FEM) to study the possible modelling procedures in low-velocity impact (LVI) and failure mechanism of carbon fiber reinforced polymer (CFRP) composite laminate of CCF300/epoxy and its structural responses. In finite element calculation, a proposed three-dimensional progressive damage model is used to determine the intralaminar damage, whereas the cohesive contact formulation is employed to analyse the interlaminar damage. The failure model performances are validated and verified based on different boundary conditions while maintaining the impact energy. Through simulation, the variation in boundary conditions significantly changes the structural responses and energy absorption of the laminates. It is hoped this study will be a great tool in determining the different composite impact scenarios.

Keywords: *Low-velocity impact (LVI); carbon fiber reinforced polymer (CFRP); finite element model (FEM); intralaminar damage; interlaminar damage*

ISSN 1823-5514, eISSN2550-164X

Received for review: 2019-08-20
Accepted for publication:2019-10-24
Published:2020-07-15

Introduction

In many engineering applications such as aerospace, marine, defence and automotive, composite structures are highly utilized for many purposes due to its superior quality of lightweight and high strength to weight ratio. Besides having such great advantages, a major drawback that degrades the supremacy of this material is low resistance toward impact loading. A low-velocity impact (LVI) is one of the loading scenarios which can cause a significant reduction in stiffness and strength of the composite structures [1]. The detection of this type of failure is quite intricate because the damage cannot be easily observed from the surface of components by the naked eyes, thus exposing the structures into great danger. For this reason, a high number of researchers focusing on low-velocity impact, and investigated in form of experiment [2,3], simulations [4–6] and a combination of both approaches [7–10].

During the LVI process in composite laminates, most experimental works referred to ASTM D7136 standard [11] for dimensioning and other related information. In most literature, the standard size of the laminates used was 150 mm x 100 mm with a cut-out rectangular support base of 125 mm x 75 mm. However, there also several kinds of literature adopted different geometry of the laminates as well as non-standard support fixture. Liu and Liao [8] used a 100 mm x 100 mm composite plate together with top and bottom cut-out support fixtures. They tested plastic fiber-reinforced polymer matrix laminate.

For the sake of cost-saving, researchers decided to shift to virtual testing using finite element method (FEM). To minimize the computational time, boundary conditions (i.e. clamping zone) and lay-up arrangement, especially at the interface between layers were crucially emphasized in the FE model. Full-scale geometry, including gripping areas, was modelled explicitly as described in the paper [9], [2], and [12]. All paper used cohesive elements to capture the onset and propagation of delamination. Other researchers such as Long et al. [13] simplified the clamping areas so that the calculation can be made faster and also acceptable results. They clamp the areas different between laminate and cut-out regions on both sides.

For the completeness of the modelling strategy in the LVI process, failure initiation and progression need to be predicted in a proper way through the implementation of the progressive damage model for composite laminates, which include damage criteria and evolution law. In previous research works, three dimensional (3D) Hashin failure criteria [14] have extensively used as initiation criteria to detect the failure, especially for uni-directional (UD) composite laminates because of its credibility to isolate different mode of failures. Long et al. [13] and Tie et al. [15] performed the failure analysis of the LVI using Hashin formulation and linear degradation scheme for progression law. Another researcher like Tie et al. [2] predicted the failure in

laminates due to impact loading using Hashin criteria together with continuum damage mechanics (CDM) degradation law. They conclude that this combination agrees well with test results.

Although the above researchers have analysed many aspects of modelling techniques in low-velocity impact through experiment and numerical simulations, the proper process guideline needs to be emphasized especially in establishing the boundary condition and implementation of progressive damage law in impact laminates. In addition, no universal damage initiation criteria that can represent all types of loading and hence leads to many researches that still introduced new approaches including this publication. Since the prior research in this area was inconclusive, this article aims to provide the details of clamping approaches (boundary condition) and failure prediction approach where the performance of the proposed model was compared between experimental data and the simulation. Three boundary conditions were used to study the effect of simplification of clamping areas together with Puck failure criteria to predict the intralaminar damage in the laminates for such type of loading. Prediction of delamination is achieved via the implementation of cohesive contact formulation which also used bilinear traction function as embedded in Abaqus software. It is hoped that the methodology proposed in this article can be a great design tool for more realistic composite parts and structures in the case of LVI.

Methods

Finite Element Modelling

The impact test was simulated using the FE method in Abaqus/Explicit platform. The laminates were produced from CCF300/epoxy composite material. The laminate material properties were summarized in Table 1, while experimental data was obtained from the publication of Han et al. [7]. The laminate consists of $[45/0/-45/90]4_s$ stacking sequences with a total thickness of 4 mm. To reduce the computational time, the global-local approach was employed where the layup arrangement was modified and rearranged according to $[45_4/0_4/-45_4/90_8/-45_4/0_4/45_4]$ stacking sequence. For this configuration, only six cohesive interfaces required. The layup modification can be viewed in Figure 1, while the interfacial properties are shown in Table 2. The intralaminar region meshed with eight-node linear brick reduced integration elements (C3D8R). To capture the damage pattern effectively, the region nearby impacted areas was modelled with finer mesh size compare with areas further away from the impacted zone.

Besides that, the impactor (ball) was modelled based on the analytical rigid body using the rigid element type (R3D4) because the stiffness of the steel ball is much higher than CFRP laminate. The diameter of the impactor is

16 mm having a mass of 5.36 kg which was applied to the model using reference point (RP) of the rigid body. The impactor was constrained in the translational degree of freedom *x*- and *y*-axes and rotational degree of freedom in all directions. The initial velocity was applied in *z*-direction through RP of the body and later is used to extract the result for contact force between the impactor and the laminate.

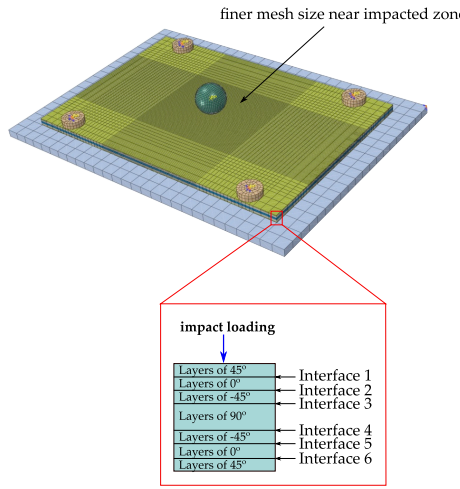

Figure 1: Local-global approach in defining the stacking sequences and meshing strategy for the LVI plate.

Table 1: The Mechanical Properties of CCF300/epoxy [7]

Category	Properties
Elastic	E_1= 123.91 GPa, E_2= E_3 = 9.72 GPa, G_{12} = G_{13} = 4.53 GPa, G_{23} = 2.56 GPa, v_{12} = v_{13} = 0.288, v_{23} = 0.347
Strength	X_t = 1762.3 MPa, X_c = 1362.2 MPa, Y_t = 71.1 MPa, Y_c = 218.3 MPa, S_{12}= S_{13} = S_{23} = 83.5 MPa
Density	ρ = 1.5 x 10^{-9} tonne/mm^3

Table 2: The Cohesive Properties of CCF300/epoxy [7]

$K_{nn} = K_{ss} = K_{tt}$	$t_n^o = t_s^o = t_t^o$	G_n^c	G_s^c= G_t^c
1 x 10^5 MPa	80 MPa	556 J/m^2	1497 J/m^2

In this article, three different models that emphasizing the boundary condition of gripping/clamping zones were analysed together with the

proposed progressive damage model. The complete description of the boundary condition and the specific model developed is illustrated in Figure 2. The analysis was carried out based on the impact energy of 4.45 J/mm which produced an initial velocity of 2.577 m/s. The contact between the impactor and the laminate was defined using general contact, and "hard contact" was specified in the normal direction. Finally, the contact force-time and load-displacement curves were extracted from the output files, and the quality of the results was compared with experimental data, as well as among the simulation data itself.

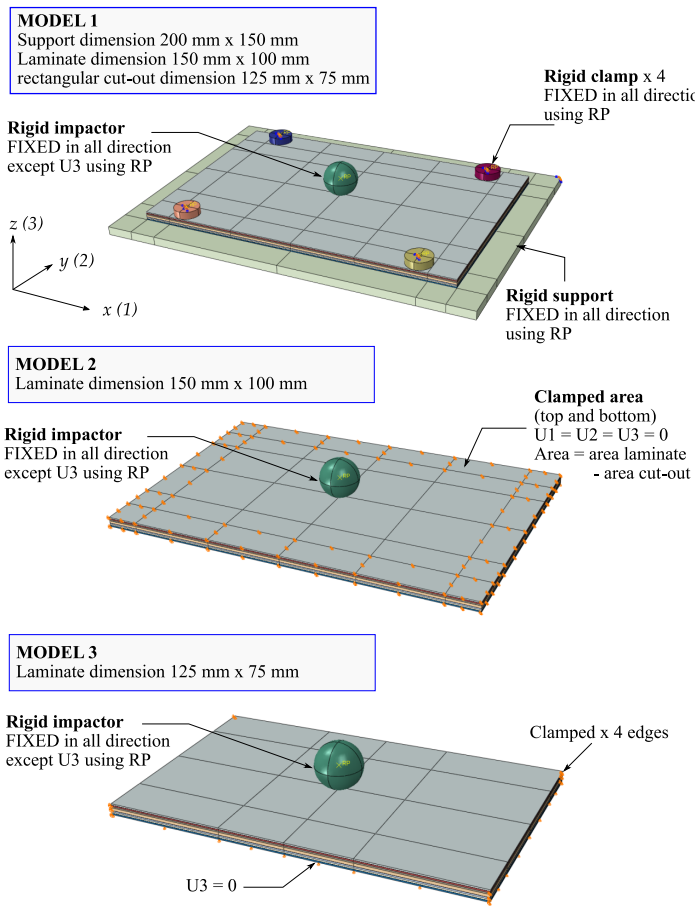

Figure 2: Different geometrical model compared in this article.

Puck's Intralaminar Damage Model

The identification and evaluation of damage initiation have been evaluated using 3D Puck failure criteria [16,17], which can distinguish fiber failure and inter-fiber failure in tension and compression. The background of this theory was extended from Hashin`s failure criteria [14]. The analytical equations represent the fiber failure (FF) in composite laminate is written in the following forms:

Fiber failure in tension:

$$f_t = \frac{1}{X_t}\left[\sigma_1 - v_{12} - v_{12f} m_{\sigma f} \frac{E_{11}}{E_{11f}} (\sigma_2 + \sigma_3)\right] \text{ for } [\ldots\ldots] \geq 0 \qquad (1)$$

Fiber failure in compression:

$$f_c = \frac{1}{|X_c|}\left[\sigma_1 - v_{12} - v_{12f} m_{\sigma f} \frac{E_{11}}{E_{11f}} (\sigma_2 + \sigma_3)\right] \text{ for } [\ldots\ldots] < 0 \qquad (2)$$

Where X_t and X_c are the tensile and compressive strengths of a UD layer in the longitudinal direction and v_{12} and v_{12f} are the Poisson's ratio for UD lamina and fibre, respectively. The mean stress magnification factor, $m_{\sigma f}$ is assumed to be 1.3 for glass fiber and 1.1 for carbon fiber [18].

For inter-fiber failure (IFF), also referred to as matrix cracking assumes that fracture in the laminate is resulted by the stresses acting on the fracture plane (FP) (σ_n, τ_{nl} and τ_{nt}) inclined θ_{FP} with respect to the material plane. The classical transformation equations are used to obtain the normal and shear stresses previously mentioned. The IFF function relies on the stresses acting on the fracture plane, and formulated as:

Inter-fiber failure in tension:

$$f_t(\theta) = \sqrt{\left(\left(\frac{1}{R_\perp} - \frac{P^+_{\perp\psi}}{R_{\perp\psi}}\right)\sigma_n(\theta)\right)^2 + \left(\frac{\tau_{nt}(\theta)}{R_{\perp\perp}}\right)^2 + \left(\frac{\tau_{nl}(\theta)}{R_{\perp\parallel}}\right)^2} + \frac{P^+_{\perp\psi}}{R_{\perp\psi}}\sigma_n(\theta) \quad \text{for } \sigma_n \geq 0 \qquad (3)$$

Inter-fiber failure in compression:

$$f_c(\theta) = \sqrt{\left(\frac{P_{\perp\psi}^{-}}{R_{\perp\psi}}\sigma_n(\theta)\right)^2 + \left(\frac{\tau_{nt}(\theta)}{R_{\perp\perp}}\right)^2 + \left(\frac{\tau_{nl}(\theta)}{R_{\perp\parallel}}\right)^2} + \frac{P_{\perp\psi}^{+}}{R_{\perp\psi}}\sigma_n(\theta) \quad \text{for } \sigma_n < 0 \tag{4}$$

The parameter ψ denotes the shear angle in action plane, $R_{\perp}$ is failure resistance normal to fibers direction, and $R_{\perp\psi}$, $R_{\perp\perp}$ and $R_{\perp\parallel}$ are the fracture resistances of the action plane due to the shear stressing.

For the sake of simplification, other parameters required to complete and calculate Equation (3) and Equation (4) were evaluated from the literature [18]. To describe the elastic-brittle behaviour of fiber-reinforced composites, a constitutive model suited for composite material was used, where Lee et al. [19] was successfully performed their numerical model to identify the onset of failure as well as damage progression. A 3D-damaged stiffness matrix is written as:

$$C^d = \begin{bmatrix} \beta C_{11} & \kappa C_{12} & \kappa C_{13} & 0 & 0 & 0 \\ \kappa C_{21} & \kappa C_{22} & \kappa C_{23} & 0 & 0 & 0 \\ \kappa C_{31} & \kappa C_{32} & \kappa C_{33} & 0 & 0 & 0 \\ 0 & 0 & 0 & \beta\omega G_{12} & 0 & 0 \\ 0 & 0 & 0 & 0 & \beta\omega G_{13} & 0 \\ 0 & 0 & 0 & 0 & 0 & \beta\omega G_{23} \end{bmatrix} \tag{5}$$

Where C_{ij} is an undamaged stiffness component, and G_{12}, G_{13} and G_{23} are the in-plane and out-of-plane shear modulus of composite material. The multiplication factors β, κ, and ω were defined as following:

$$\begin{aligned} \beta &= 1 - d_f \\ \kappa &= (1 - d_f)(1 - d_m) \\ \omega &= (1 - S_{mt}d_{mt})(1 - S_{mc}d_{mc}) \end{aligned} \tag{6}$$

Where d_f and d_m are the global damage variables corresponding to fibre and inter-fibre failure, respectively. Individual damage variables based on failure mode are represented by d_{ft}, d_{fc}, d_{mt} and d_{mc} for fibre failure in tension and compression and inter-fibre failure in tension and compression, respectively. The relationship between global and local variables is defined as $d_f = 1 - (1 - d_{ft})(1 - d_{fc})$ and $d_m = 1 - (1 - d_{mt})(1 - d_{mc})$. The control

parameters, S_{mt} and S_{mc} are 0.9 and 0.5, respectively as suggested in the Abaqus manual.

Interlaminar Damage Model

Delamination was simulated by cohesive surface behaviour using a cohesive contact interface. Based on the formulation, the fracture-separation law was employed to control the interaction between traction stress and separation displacement in the model as written in matrix form below:

$$t = \begin{bmatrix} t_n \\ t_s \\ t_t \end{bmatrix} = \begin{bmatrix} K_{nn} & 0 & 0 \\ 0 & K_{ss} & 0 \\ 0 & 0 & K_{tt} \end{bmatrix} \begin{bmatrix} \delta_n \\ \delta_s \\ \delta_t \end{bmatrix} \tag{7}$$

Where t_n, t_s and t_t are the interface strength under the failure mode I, II, and III respectively. The damage initiation and progression based on delamination mode is summarized in Table 3.

Table 3: Failure criteria for delamination

Approach	Cohesive contact interface
Damage initiation	Quadratic nominal stress criterion $\left\{\frac{\langle t_n \rangle}{t_n^o}\right\}^2 + \left\{\frac{t_s}{t_s^o}\right\}^2 + \left\{\frac{t_t}{t_t^o}\right\}^2 = 1$
Damage evolution	Power law fracture criterion $\left\{\frac{G_n}{G_n^c}\right\}^\alpha + \left\{\frac{G_s}{G_s^c}\right\}^\alpha + \left\{\frac{G_t}{G_t^c}\right\}^\alpha = 1$

From Table 3, t_i ($i = n, s, t$) is the interface strength parameters, $G_i^c (i = n, s, t)$ is the critical fracture energy needed to cause damage in the normal and two shear directions and α is the material parameter (i.e.$\alpha = 1$). The onset of delamination can be identified whenever the quadratic function achieved unity (=1). Once the damage criteria are satisfied, the cohesive stiffness degraded according to the power law.

Numerical Result and Discussion

The numerical simulation is focused on CCF300/epoxy composite with different modelling techniques on the boundary condition of clamped areas based on impact energy of 4.45 J/mm. The contact force and load-displacement

diagram were recorded for determining the performance of the proposed model and the damage model.

Analysis of Modelling Boundary Condition

This sub-section analyses the effect of boundary condition on the LVI specimen in predicting the failure in a composite laminate. The simulated impact force-time curves from 3 models are compared with the experiment curve and result in Figure 3 revealed that the duration of impact force in virtual test curves is slightly shorter than the real curve which is mainly due to the philosophy of applied boundary condition. As a comparison, model 1 and 2 are closely mimicked the test curve because of the boundary condition includes the rubber grips and cut-out support, however, over estimates the ultimate impact force. Model 3 and the proposed model of Han et al. [7] are performed better in predicting the contact force, and the simulated results agreed well with the experiment.

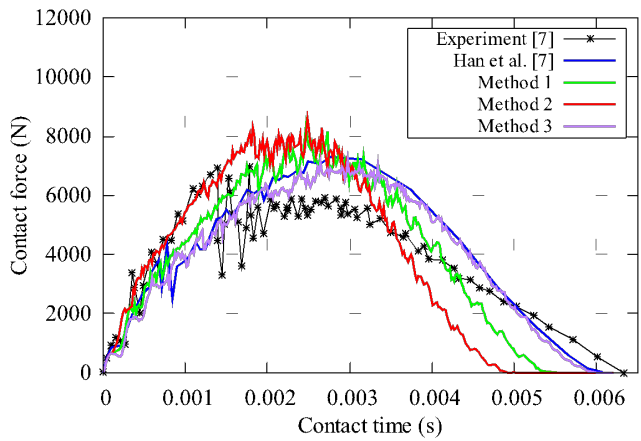

Figure 3: Comparison of simulation and experimental data for contact force vs time of CCF300/epoxy laminate.

Figure 4 shows the force-displacement curve for the models investigated in this paper. Because of no reference on the force-displacement curve from the experiment, the comparison is only made based on these three models. The prediction of the load-displacement curve shows a similar pattern in all cases where model 1 and model 3 gave better results in producing lower energy absorption. Model 3 can be used as an optimized tool to reduce the calculation time and at the same time produced reasonable results. Model 1 used less time to bounce back the impactor and utilized low kinetic energy as compared to other models.

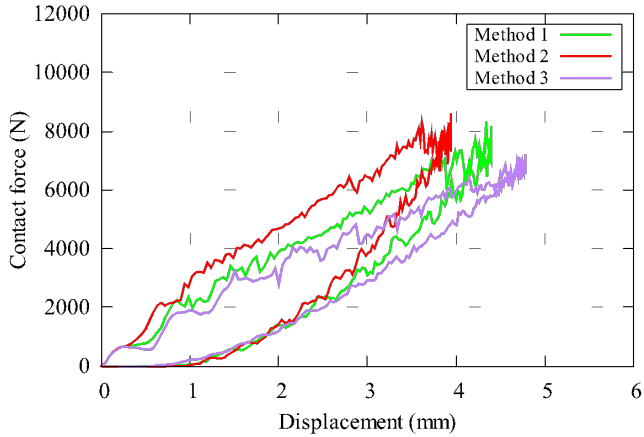

Figure 4: Simulated force-displacement of CCF300/epoxy LVI laminate under model 1, 2 and 3

Table 3 demonstrates the performance of models in absorbing the impact energy. Results indicated that Model 2 absorbed the highest energy compare to the other two models due to the nature of the clamped areas which was bigger than model 1. The structure becomes more rigid and causes higher energy required to bounce back the impactor. Model 3 utilized only an "edge line" for the un-supported laminate, which produced lower energy value.

Table 3: Analysis of energy absorption for proposed models based on impact energy of 4.45 J/mm

Model	Energy absorbed (J)
Model 1	7.883
Model 2	9.276
Model 3	6.535

Analysis of Damage Initiation and Growth

With the impact energy of 4.45 J/mm selected in this analysis, only matrix failure observed as shown in Figure 5. Red/dark color indicates full damage, while other colors exhibit no failure area. Matrix damage radius increases for matrix failure in tension measured from impacted point to the bottom layer of the laminates, while decreases for compressive matrix failure. These trends similarly observed in the original publication [7]. The failure in fiber modes is not observed here due to the inadequate impact energy applied to the composite plate that can break the fiber inside it.

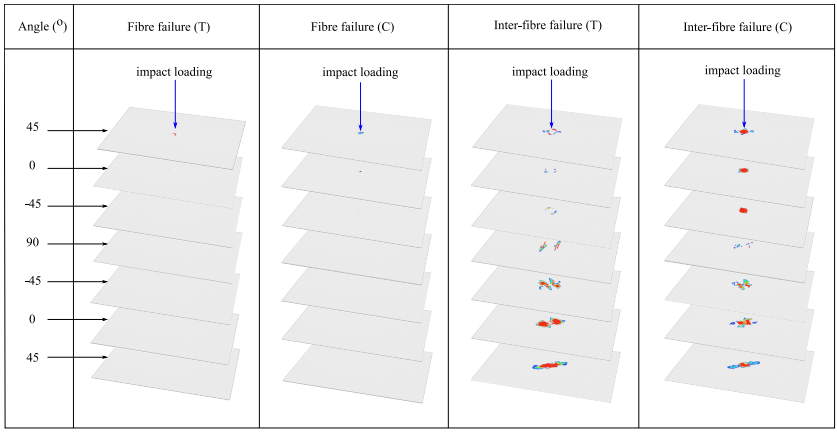

Figure 5: Intralaminar morphology for the impact energyof 4.45 J/mm (for Model 1)

Delamination or debonding is another area of interest in predicting total failure due to impact loading. As can be seen in Figure 6, the damage morphology indicates the area of delamination getting bigger towards the 90° layups, and slowly decreases approaching the last bottom layers. The existence of delamination boosts the process of damage accumulation by degrading the stiffness of the laminate.

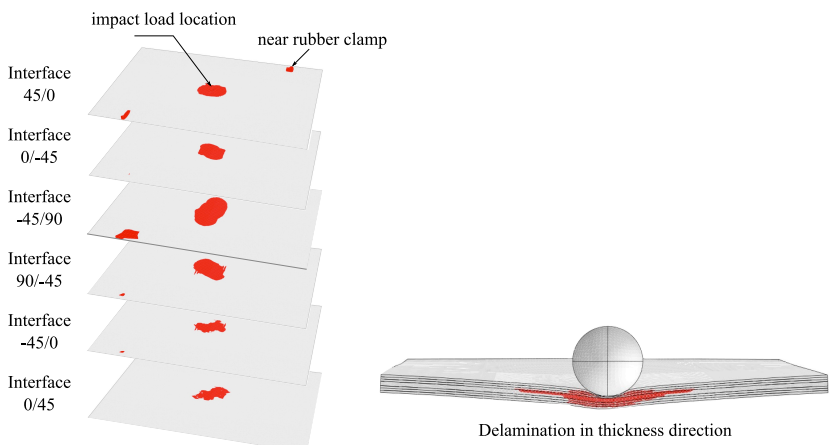

Figure 6: Delamination morphology for the impact energy of 4.45 J/mm (Model 1) (red/dark color defines the failure area)

Conclusions

In this paper, Puck damage criteria incorporated with a gradual degradation scheme and cohesive damage formulation were proposed to study the failure mechanism of fiber and matrix components as well as the structural response of CCF300/epoxy composite laminate subjected to low-velocity impact loading. The damage model is used to study the damage morphology, as well as the force-displacement response of the impactor. The cohesive theory is applied to the FE model to detect and trace the phenomena of delamination. Based on the simulations conducted, it has been concluded that:

- In general, the proposed damage model can predict the contact force and damage failure modes consistently with the test result.
- The full-scale FE model (model 1) has performed excellently in capturing the structural response, while satisfactorily predict the peak force. Since no information obtained from the experiment, further comparison cannot be made regarding on efficiency of the load-displacement curve.
- Due to the inadequate magnitude of impact energy, no trace of fiber failure (FF) can be viewed in the analysis of results. Matrix failures are the main contributor to the total failure in the laminate for LVI structure.
- The low-velocity impact results in the delamination in all sub-laminate, which varies in terms of areas based on the location from the impacted point.

References

[1] Yang L, Wu Z, Gao D, Liu X., "Microscopic damage mechanisms of fibre reinforced composite laminates subjected to low velocity impact," Computational Materials Science 111, 148–156 (2016).

[2] Tie Y, Hou Y, Li C, Zhou X, Sapanathan T, Rachik M., "An insight into the low-velocity impact behavior of patch-repaired CFRP laminates using numerical and experimental approaches," Composite Structures 190, 179–188 (2018).

[3] Gliszczynski A., "Numerical and experimental investigations of the low velocity impact in GFRP plates," Composites Part B: Engineering 138, 181–193 (2018).

[4] Perillo G, Vedvik NP, Echtermeyer AT., "Numerical analyses of low velocity impacts on composite. Advanced modelling techniques," In: Proceedings of the Simulia customer conference (2012).

[5] Zhang J, Zhang X. "An efficient approach for predicting low-velocity impact force and damage in composite laminates," Composite Structures.130, 85–94 (2015).

[6] Maio L, Monaco E, Ricci F, Lecce L., "Simulation of low velocity impact on composite laminates with progressive failure analysis," Composite Structures 103, 75–85 (2013).
[7] Han G, Guan Z, Li X, Du S., "Failure analysis of carbon fiber reinforced composite subjected to low velocity impact and compression after impact.," Journal of Reinforced Plastics and Composites 35(9), 727-746 (2016).
[8] Liu PF, Liao BB, Jia LY, Peng XQ, "Finite element analysis of dynamic progressive failure of carbon fiber composite laminates under low velocity impact," Composite Structures 149, 408–422 (2016).
[9] Lou X, Cai H, Yu P, Jiao F, Han X., "Failure analysis of composite laminate under low-velocity impact based on micromechanics of failure," Composite Structures 163 (2017).
[10] Singh H, Namala KK, Mahajan P., "A damage evolution study of E-glass/epoxy composite under low velocity impact," Composites Part B: Engineering (2015).
[11] D7136 A., "Standard Test Method for Measuring the Damage Resistance of a Fiber-Reinforced-Polymer Matrix Composites to a Drop-Weight Impact event," Book of Standards 15 (2005).
[12] Riccio A, De Luca A, Di Felice G, Caputo F., "Modelling the simulation of impact induced damage onset and evolution in composites," Composites Part B: Engineering 66, 340–347 (2014).
[13] Long S, Yao X, Zhang X., "Delamination prediction in composite laminates under low-velocity impact," Composite Structures 132, 290–298 (2015).
[14] Hashin Z., "Fatigue Failure Criteria for Unidirectional Fiber Composites," Journal of Applied Mechanics 48(4), 846 (2009).
[15] Du J, Tie Y, Li C, Zhou X., "Numerical and experimental study for damage characterization of composite laminates subjected to low-velocity impact," Materials Physics and Mechanics 27(2), 195–204 (2016).
[16] Puck A., "Failure Analysis of FRP Laminates By Means of Physically Based Phenomenological Models," Composites Science and Technology 58(7), 1045–1067 (1998).
[17] Puck A, Deuschle HM., "Progress in the Puck Failure Theory for Fibre Reinforced Composites : Analytical solutions for 3D-stress," Composites Science and Technology 62, 371–378 (2002).
[18] Puck A, Kopp J, Knops M., "Errata to 'Guidelines for the determination of the parameters in Puck's action plane strength criterion," Composites Science and Technology 62(9), 1275 (2002).
[19] Lee CS, Kim JH, Kim SK, Ryu DM, Lee JM., "Initial and progressive failure analyses for composite laminates using Puck failure criterion and damage-coupled finite element method," Composite Structures 121(0), 406–419 (2015).